Biochemical and Biophysical Research Communications 452 (2014) 817–821

Contents lists available at ScienceDirect

Biochemical and Biophysical Research Communications

journal homepage: www.elsevier.com/locate/ybbrc

Fast conformational exchange between the sulfur-free and persulfide-bound rhodanese domain of *E. coli* YgaP

Wei Wang [a], Peng Zhou [b], Yao He [a], Lu Yu [a], Ying Xiong [a], Changlin Tian [a,b,*], Fangming Wu [b,*]

[a] Hefei National Laboratory for Physical Sciences at the Microscale and School of Life Sciences, University of Science and Technology of China, Hefei, Anhui 230026, PR China
[b] High Magnetic Field Laboratory, Chinese Academy of Sciences, Hefei, Anhui 230031, PR China

ARTICLE INFO

Article history:
Received 19 August 2014
Available online 7 September 2014

Keywords:
Rhodanese domain
Solution NMR
Three-dimensional structure
Sulfur transfer
Fast conformational exchange
Chemical shift perturbation

ABSTRACT

Rhodanese domains are abundant structural modules that catalyze the transfer of a sulfur atom from thiolsulfates to cyanide via formation of a covalent persulfide intermediate that is bound to an essential conserved cysteine residue. In this study, the three-dimensional structure of the rhodanese domain of YgaP from *Escherichia coli* was determined using solution NMR. A typical rhodanese domain fold was observed, as expected from the high homology with the catalytic domain of other sulfur transferases. The initial sulfur-transfer step and formation of the rhodanese persulfide intermediate were monitored by addition of sodium thiosulfate using two-dimensional ^{1}H–^{15}N correlation spectroscopy. Discrete sharp signals were observed upon substrate addition, indicting fast exchange between sulfur-free and persulfide-intermediate forms. Residues exhibiting pronounced chemical shift changes were mapped to the structure, and included both substrate binding and surrounding residues.

1. Introduction

Rhodanese was first reported in 1933 as an enzyme capable of catalyzing the transfer of a sulfur atom from thiosulfate to the toxic cyanide, resulting in the non-toxic thiocyanate [1]. The cyanide detoxification activity of rhodanese has since been identified in all three major evolutionary phyla [2], and the enzyme has been given the full name thiosulfate:cyanide sulfurtransferase (TST, EC 2.8.1.1) [3]. Rhodanese domains are found as tandem repeats, single domain proteins or in combination with distinct protein domains [4].

The best-characterized are the mitochondrial bovine TST (Rhobov) [5,6] and the *Azotobacter vinelandii* rhodanese (RhdA) enzymes [7], both of which contain two tandem rhodanese domains and an essential conserved Cys residue in the C-terminal rhodanese domain that is critical for catalysis. It has been reported that lack of the Cys residue in the N-terminal rhodanese domain also results in an inactive enzyme [5,7]. Structurally, rhodanese domains are closely related to the human phosphatase Cdc25, both in tertiary structure and the location of the conserved Cys [8,9]. In *Escherichia coli*, eight proteins have been identified as containing rhodanese domains [10], and three (GlpE, PspE, and YgaP) belong to the single-domain rhodanese homology family and contain the essential Cys [11]. Among them, YgaP is the only membrane-associated rhodanese with the predicted two transmembrane helices near the C-terminus [12].

Currently, two separate sulfur-transfer steps are believed to occur during catalysis. In the first step, the sulfhydryl (−SH) group of the conserved Cys residue attacks the thiosulfate ($S_2O_3^{2-}$) anion, forming a covalent persulfide intermediate; in the second step, the persulfide intermediate is attacked by a cyanide (CN^-) ion to release the thiocyanate (SCN^-) product and regenerate the cysteine sulfhydryl group [3,7]. The three-dimensional structure of PspE was determined using solution NMR. It was reported that backbone dynamics of the persulfide intermediate of PspE was less stable and more conformationally flexible than the ligand-free form, despite of similar conformations between the two forms [13].

In this work, we determined the NMR solution structure of the rhodanese domain of YgaP from *E. coli*. The structure showed a typical fold reminiscent of GlpE [11] and PspE [13]. During preparation of this communication, Eichmann et al. [14] reported the solution NMR structure of full-length YgaP in the presence of detergent micelles, which formed a homo-dimer with strong hydrophobic interactions between the two transmembrane helices of each subunit, although no direct interactions between the N-terminal rhodanese domains were visible. The YgaP rhodanese domain structure determined in the present study was highly similar to full length YgaP. Formation of the persulfide intermediate resulting

* Corresponding authors. Address: Hefei National Laboratory for Physical Sciences at the Microscale and School of Life Sciences, University of Science and Technology of China, Hefei, Anhui 230026, PR China (C. Tian).
E-mail addresses: cltian@ustc.edu.cn (C. Tian), fmwu@hmfl.ac.cn (F. Wu).

http://dx.doi.org/10.1016/j.bbrc.2014.09.002
0006-291X/

from the first sulfur-transfer step was monitored using two dimensional NMR following addition of sodium thiosulfate. Interestingly, significant chemical shift perturbations were observed in both substrate binding and surrounding residues. Line shape analysis indicated that a fast exchange takes place between the ligand-free and persulfide-bound forms.

2. Materials and methods

2.1. Protein preparation

The DNA sequence encoding the rhodanese domain of YgaP (residues 1–107) from *E. coli* was cloned into the expression vector p28 (modified from pET-28a, Novagen) to include an N-terminal 6× His tag. The recombinant protein $YgaP_{1\text{-}107}$ was expressed in *E. coli* host strain BL21-Gold(DE3) in M9 media and induced with 0.4 mM IPTG at 37 °C for 5 h. Isotopically enriched proteins were prepared using $^{15}NH_4Cl$ (1 g/L) and ^{13}C-D-glucose (2.5 g/L) (Cambridge Isotope Laboratories) as the sole nitrogen and carbon sources, respectively. Expressed proteins were purified using Ni–NTA resin (Qiagen). The final NMR sample consisted of 0.5 mM $YgaP_{1\text{-}107}$ in 20 mM Tris–HCl pH 7.0, 20 mM NaCl in a 90% H_2O/10% D_2O mixture, or in 100% D_2O.

2.1.1. NMR spectra and structure determination

A standard set of multiple resonance NMR spectra including 2D $^1H/^{15}N$-HSQC, 3D CBCA(CO)NH, HNCACB, HNCO, C(CO)NH, HBHA(CO)NH, H(CCO)NH, HCCH-TOCSY, HCCH-COSY, ^{15}N-edited NOESY (mixing time 80 ms) and ^{13}C-edited NOESY (mixing time 150 ms) were recorded using a Varian 700 MHz spectrometer. NMR data were processed using NMRPipe [15] and analyzed with Sparky [16]. Backbone torsion angle restraints were predicted from assigned chemical shifts ($^{13}C\alpha$, $^{13}C\beta$, ^{13}CO, $^1H\alpha$, ^{15}N, ^1HN) using the TALOS+ program [17]. The resulting dihedral angle and NOE restraints were applied in structure calculation of $YgaP_{1\text{-}107}$ using Xplor-NIH [18]. Finally, 10 structures with the lowest energy were selected from 100 calculated structures, and the quality was assessed using PROCHECK-NMR [19] and MOLMOL [20].

2.1.2. Monitoring persulfide intermediate formation by solution NMR

^{15}N-labeled $YgaP_{1\text{-}107}$ (20 mM Tris pH 7.0, 50 mM NaCl, 0.5 mM $YgaP_{1\text{-}107}$) was used in the NMR titration experiment. A 50 mM stock solution of $Na_2S_2O_3$ and NaSCN were also prepared in the same buffer as $YgaP_{1\text{-}107}$. Several $^1H/^{15}N$-HSQC spectra were recorded using a Varian 700 MHz spectrometer, with the following $Na_2S_2O_3/YgaP_{1\text{-}107}$ (or NaSCN/$YgaP_{1\text{-}107}$) molar ratios: 0:1, 0.2:1, 0.5:2, 2:1, 5:1, and 10:1. Potential binding residues were determined from the chemical shift perturbation (CSP) data calculated using formula (1),

$$\mathrm{CSP} = \sqrt{\Delta H^2 + \left(\frac{\Delta N}{5}\right)^2} \quad (1)$$

where ΔH and ΔN are the chemical shift differences between the backbone H and N atoms of the ligand-free and ligand-bound form.

The dissociation constant (Kd) of the interaction for the fast exchange binding process was estimated by curve fitting using the one-site-binding model as in formula (2),

$$Y = \frac{B_{\max} \times X}{K + X} \quad (2)$$

where X is the concentration of the substrate ($Na_2S_2O_3$), $B_{\max}$ is the maximum CSP when substrate concentration is ∞, K is the dissociation constant, and Y is the CSP.

3. Results and discussion

3.1. Overall structure of the YgaP rhodanese domain

Approximately 98% of backbone resonances ($^{13}C\alpha$, ^{13}CO, ^1HN, and ^{15}N) and 98% of side chain resonances (^1H) were assigned, excluding those of the 6× His-tag. A $^1H/^{15}N$-HSQC spectra with peaks assigned is shown in Supplementary Fig. S1. The structure of $YgaP_{1\text{-}107}$ was determined on the basis of 1998 restraints, including 1872 inter-proton distance restraints, and 126 dihedral angle restraints. The 10 lowest energy structures were selected out of 100 calculated structures, and the statistics on model quality are summarized in Table 1. The backbone superimposition of the final 10 conformers and representative structures are presented in Fig. 1A and B.

The overall structure of the rhodanese domain of $YgaP_{1\text{-}107}$ adopted the α–β–α sandwich fold typical of a rhodanese domain, with a central five-stranded parallel β-sheet (β1, residues 4–6; β2, residues 20–22; β3, residues 39–40; β4, residues 59–63; β5, residues 86–89) surrounded by five α-helices (α1, residues 8–16; α2, residues 27–32; α3, residues 43–48; α4, residues 68–80; α5, residues 93–98) and a 3_{10} helix (residues 53–55) on both sides (Fig. 1B). The structural topology was generated by PDBsum [21] and is shown in Supplementary Fig. S2.

The catalytic residue Cys64 is located at the edge of β4 of the central five-stranded parallel β-sheet, and is surrounded by four α-helices (α2–α4) (Fig. 1B) that form a cavity in which substrate binds and sulfur-transfer takes place. Cys64 is the first residue of the 6-residue loop (Cys64–Arg69) between β4 and α4 that forms a cradle-like semi-circular structure, with the catalytic Sγ atom located at the geometrical center of the substrate binding pocket. Backbone amide protons of residues Gln65-Arg69 all point towards the Cys64-Sγ (Fig. 1C). The electrostatic potential surface of $YgaP_{1\text{-}107}$ showed that the active site pocket is guarded by a positively charged bulb (Lys68 and Arg69) and a negatively charged bulb (Asp26, Asp28 and Glu29) (Supplementary Fig. S3).

3.2. Structural comparison of rhodanese domains

A total of eight rhodanese domain-containing proteins are encoded in the *E. coli* genome [11], and three-dimensional structures of three of these (GlpE, PDB code 1GMX; PspE, PDB code 2JTQ; YgaP, PDB code 2MRM) contain a single rhodanese domain

Table 1
Structural statistics for the final 10 conformers of the rhodanese domain of YgaP from *E. coli*.

Number of distance constrains	
NOE distance constraints	1872
Intraresidue ($i - j = 0$)	345
Sequential ($i - j = 1$)	552
Medium-range ($2 \leqslant i - j \leqslant 4$)	456
Long-range ($i - j \geqslant 5$)	519
Number of dihedral angle constraints	126
Rmsd for experimental restraints	
NOE distance constraints	0.009 ± 0.001
Dihedral angle constraints	0.222 ± 0.042
Rmsd from idealized covalent geometry	
Bonds (Å)	0.001 ± 0.000
Angles (°)	0.395 ± 0.004
Impropers (°)	0.237 ± 0.006
Average RMSD of atomic coordinates (Å)	
Backbone atoms (secondary structure region)	0.435
All heavy atoms (secondary structure region)	0.965
Ramachandran plot analysis (%)	
Most favorable region	80
Additional allowed regions	16.1
Generously allowed regions	2.9
Disallowed regions	1.0

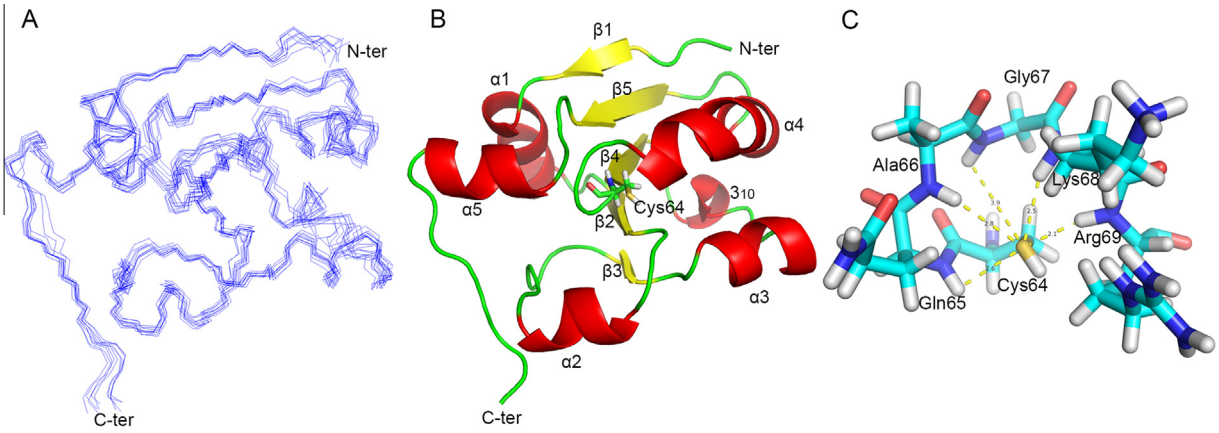

Fig. 1. Solution NMR structure of the rhodanese domain of YgaP. (A) Backbone superposition of the final 10 conformers. N- and C-termini are labeled. (B) Cartoon representation of the structure of $YgaP_{1\text{-}107}$. N- and C-termini, secondary structural elements and the catalytic residue Cys64 are labeled. (C) Detailed structure of the active site.

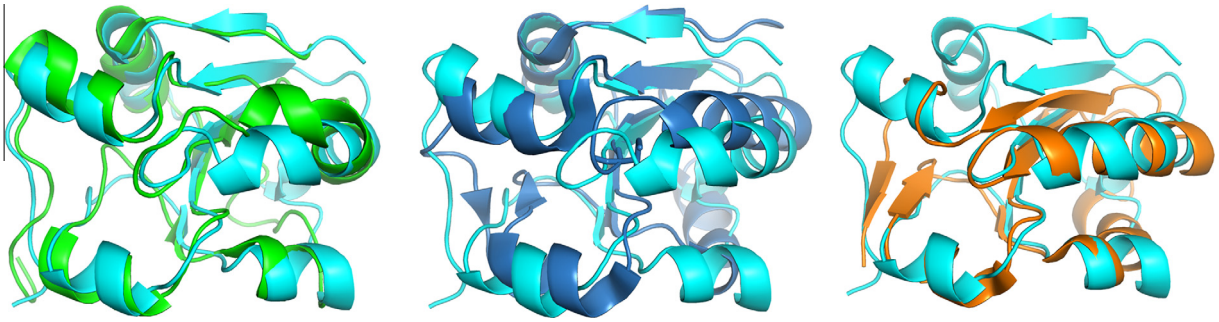

Fig. 2. Structural comparison of three rhodanese domains from *E. coli*: superimposition of our NMR structure of YgaP (Cyan, PDB code 2MRM), the NMR structure of YgaP by Eichmann et al. (Green, PDB code 2MOI), the crystal structure of GlpE (skyblue, PDB code 1GMX), and the NMR structure of PspE (Orange, PDB code 2JTQ). (For interpretation of the references to color in this figure legend, the reader is referred to the web version of this article.)

[3,22]. Sequence alignment of these rhodanese domains using Clustal Omega [23] and processed with ESPript 3.0 (http://espript.ibcp.fr) [24] revealed only very low sequence homology between the amino acid sequences (Supplementary Fig. S4). The YgaP rhodanese domain shared 23% and 25% sequence identity with GlpE and PspE, respectively. Conserved sequence regions are highlighted by magenta boxes and labeled I, II, and III (Supplementary Fig. S4). Sequence I lies at the end of β2, next to the active site Cys64. Sequence II corresponds to the first of the two so-called 'rhodanese signatures' [3], and Sequence III is the substrate binding loop.

Structural alignment of the three rhodanese domains showed high structural similarity despite the low sequence identity (Fig. 2 and Supplementary Fig. S4). Some minor structural differences were apparent, including an extra two-stranded anti-parallel β-sheet (formed from residues of the C-terminus and between α2 and β3) in GlpE and PspE that is absent in $YgaP_{1\text{-}107}$ (Fig. 2). Additionally, the first α-helix and β-strand were absent in the NMR structure of PspE [13], and the α3 in GlpE and PspE is much longer than the equivalent short α-helix and 3_{10} helix in YgaP (Fig. 2). The solution NMR structure was also superimposed with that determined by Eichmann et al. [14], and the two structures were highly similarity, with a DaliLite Z-score [25] of 13.5 and an RMSD value of 2.0 in a pairwise structure alignment (Fig. 2).

3.3. Fast conformational exchange between the ligand-free and persulfide-bound YgaP rhodanese domain

In the enzymatic reaction, TSTs (thiosulfate:cyanide sulfurtransferases) use thiosulfate ($S_2O_3^{2-}$) as substrate and catalyze the transfer of a sulfur atom to the sulfur acceptor cyanide (CN^-) to form the product thiocyanate (SCN^-) [4,7]. Two separate sulfur-transfer steps have been reported. In the first step, a persulfide intermediate is formed by attack of the active site Cys-SH group (Cys64 in YgaP) on the thiosulfate anion substrate.

Previously, solution NMR structure analysis demonstrated similar conformations for ligand-free enzyme and the covalent persulfide intermediate of *E. coli* PspE [13], and backbone dynamic analysis indicated a rapid chemical exchange in residues surrounding the essential cysteine residue.

In this study, the first sulfur-transfer reaction from the thiosulfate anion to the cysteine residue was monitored using two-dimensional $^1H–^{15}N$ correlation HSQC spectroscopy, using increasing increments of the substrate sodium thiosulfate ($Na_2S_2O_3$). A total of six HSQC spectra with different molar ratios of $Na_2S_2O_3$ to $YgaP_{1\text{-}107}$ (0:1, 0.2:1, 0.5:1, 2:1, 5:1, 10:1) were acquired and processed. Although the overlaid HSQC spectra demonstrated a highly similar resonance distribution pattern, significant chemical shift changes were apparent for several resonances in three different regions: 25–41, 64–72, 90–95 (Fig. 3A–D). The observed chemical shift differences strongly indicated that there were conformation changes between the persulfide intermediate and the ligand-free enzyme, especially in residues with pronounced chemical shift changes.

Enzymatic reaction should normally result in a new product (persulfide-SSH rather than Cys-SH), and different NMR signals or chemical shift values should be observed for Cys-SSH and the surrounding residues. Theoretically, with increasing substrate concentration, two NMR signals with conjugated intensity changes should

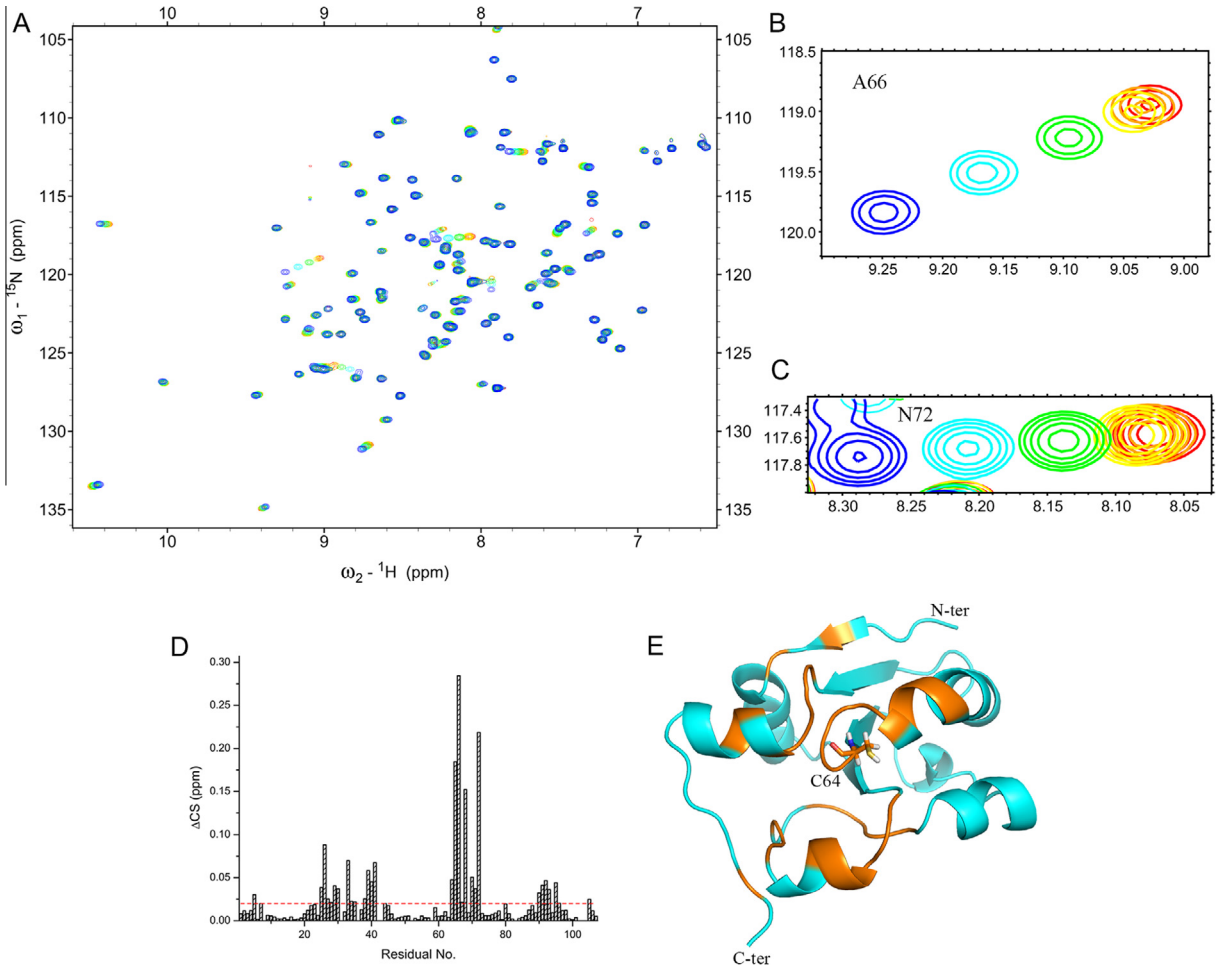

Fig. 3. Two-dimensional heteronuclear $^{1}H–^{15}N$ correlation spectra recorded in the presence of different molar ratios of $Na_2S_2O_3$ substrate and $YgaP_{1\text{-}107}$ (A). The chemical shift changes of residues Ala66 (B) and Asn72 (C) upon the addition of $Na_2S_2O_3$ are enlarged for clarity. Different colors correspond to different $Na_2S_2O_3$/YgaP ratios as follows: red (0:1), orange (0.2:1), yellow (0.5:1), green (2:1), cyan (5:1), blue (10:1). (D) CSP values of all residues plotted against residue number. The red dashed line indicates a CSP of 0.02 ppm. (E) Chemical shift changes of residues of $YgaP_{1\text{-}107}$ upon titration with sodium thiosulfate mapped onto the solution NMR structure of $YgaP_{1\text{-}107}$. Orange: perturbed residues with CSP larger than 0.02 ppm; Cyan: residues with CSP lower than 0.02 ppm. (For interpretation of the references to color in this figure legend, the reader is referred to the web version of this article.)

be observed for residues directly involved in catalysis, with one peak decreasing and the other increasing in intensity as the reaction proceeds. However, no such conjugated peak intensity changes were observed for Ala66 or Asn72 with increasing $Na_2S_2O_3$ (Fig. 3B and C), and there were no conjugated peak intensity changes observed in overlaid HSQC spectra either (Fig. 3A). This strongly indicated that fast conformational exchange occurs between the ligand-free and persulfide-bound forms [26]. Other residues showed markedly large chemical shift changes (Cys64, Lys68, Thr70, and Ser71; Supplementary Fig. S5), and these residues all reside in the active-site loop and surrounding region, which highlights the precise region in which the catalytic reaction takes place.

3.4. Residues exhibiting pronounced chemical shift perturbations in YgaP

During the chemical shift perturbation analysis of $YgaP_{1\text{-}107}$ with increasing $Na_2S_2O_3$, several resonances were significantly perturbed (Fig. 3A), especially the active site loop region (Cys64-Asn72). Additionally, chemical shifts of residues from the adjacent two loops connecting β2 and α2, and β5 and α5, were also perturbed upon addition of substrate. This result implies extensive binding interactions between the enzyme (YgaP) and the substrate ($Na_2S_2O_3$). Chemical shift perturbations for each residue were plotted against residue number (Fig. 3D), and Thr5, Ser7, Arg25–Tyr30, Glu33–Ile35, Ala38–Ala41, Cys64–Lys68, Thr70–Asn72, Glu90–Ile93, Gly95–Trp96, and Val105 were all perturbed significantly (CSP $\geqslant$ 0.02 ppm). These residues were visualized on the three-dimensional structure of $YgaP_{1\text{-}107}$ (Fig. 3E). Using the chemical shift changes of Ala66 and Asn72 (Fig. 3B and C), the dissociation constant (Kd) was calculated to be around 6.8 mM by data fitting (Supplementary Fig. S6).

In summary, we determined the solution NMR structure of the rhodanese domain of YgaP from *E. coli*. The substrate concentration-dependent chemical shift changes indicated that a rapid conformational exchange occurs between ligand-free and persulfide-bound forms.

4. Accession numbers

Coordinates of the rhodanese domain of YgaP have been deposited in the Protein Data Bank under ID code 2MRM. Chemical shifts of $YgaP_{1\text{-}107}$ have been deposited in BioMagResBank with accession number 25085.

Conflict of interest statement

All authors declare no conflict of interests.

Acknowledgments

This work was supported by funds from the Ministry of Science and Technology of China (Grant Numbers 2012CB917202 and 2013CB910200), and Projects 31100538, 31100847 and 31470740 of the National Natural Science Foundation of China.

Appendix A. Supplementary data

Supplementary data associated with this article can be found, in the online version, at http://dx.doi.org/10.1016/j.bbrc.2014.09.002.

References

[1] K. Lang, Die rhodanbildung in tierkorper, Biochem. Z. 259 (1933) 243–256.
[2] J. Westley, H. Adler, L. Westley, C. Nishida, The sulfurtransferases, Fundam. Appl. Toxicol. 3 (1983) 377–382.
[3] R. Cipollone, P. Ascenzi, P. Visca, Common themes and variations in the rhodanese superfamily, IUBMB Life 59 (2007) 51–59.
[4] D. Bordo, P. Bork, The rhodanese/Cdc25 phosphatase superfamily. Sequence-structure-function relations, EMBO Rep. 3 (2002) 741–746.
[5] J.H. Ploegman, G. Drent, K.H. Kalk, W.G. Hol, R.L. Heinrikson, P. Keim, L. Weng, J. Russell, The covalent and tertiary structure of bovine liver rhodanese, Nature 273 (1978) 124–129.
[6] D.L. Nandi, P.M. Horowitz, J. Westley, Rhodanese as a thioredoxin oxidase, Int. J. Biochem. Cell Biol. 32 (2000) 465–473.
[7] D. Bordo, D. Deriu, R. Colnaghi, A. Carpen, S. Pagani, M. Bolognesi, The crystal structure of a sulfurtransferase from *Azotobacter vinelandii* highlights the evolutionary relationship between the rhodanese and phosphatase enzyme families, J. Mol. Biol. 298 (2000) 691–704.
[8] E.B. Fauman, J.P. Cogswell, B. Lovejoy, W.J. Rocque, W. Holmes, V.G. Montana, H. Piwnica-Worms, M.J. Rink, M.A. Saper, Crystal structure of the catalytic domain of the human cell cycle control phosphatase, Cdc25A, Cell 93 (1998) 617–625.
[9] R.A. Reynolds, A.W. Yem, C.L. Wolfe, M.R. Deibel Jr., C.G. Chidester, K.D. Watenpaugh, Crystal structure of the catalytic subunit of Cdc25B required for G2/M phase transition of the cell cycle, J. Mol. Biol. 293 (1999) 559–568.
[10] F.R. Blattner, G. Plunkett 3rd, C.A. Bloch, N.T. Perna, V. Burland, M. Riley, J. Collado-Vides, J.D. Glasner, C.K. Rode, G.F. Mayhew, J. Gregor, N.W. Davis, H.A. Kirkpatrick, M.A. Goeden, D.J. Rose, B. Mau, Y. Shao, The complete genome sequence of *Escherichia coli* K-12, Science 277 (1997) 1453–1462.
[11] A. Spallarossa, J.L. Donahue, T.J. Larson, M. Bolognesi, D. Bordo, *Escherichia coli* GlpE is a prototype sulfurtransferase for the single-domain rhodanese homology superfamily, Structure 9 (2001) 1117–1125.
[12] C. Tzitzilonis, C. Eichmann, I. Maslennikov, S. Choe, R. Riek, Detergent/nanodisc screening for high-resolution NMR studies of an integral membrane protein containing a cytoplasmic domain, PLoS ONE 8 (2013) e54378.
[13] H. Li, F. Yang, X. Kang, B. Xia, C. Jin, Solution structures and backbone dynamics of *Escherichia coli* rhodanese PspE in its sulfur-free and persulfide-intermediate forms: implications for the catalytic mechanism of rhodanese, Biochemistry 47 (2008) 4377–4385.
[14] C. Eichmann, C. Tzitzilonis, E. Bordignon, I. Maslennikov, S. Choe, R. Riek, Solution NMR structure and functional analysis of the integral membrane protein YgaP from *E. coli*, J. Biol. Chem. (2014).
[15] F. Delaglio, S. Grzesiek, G.W. Vuister, G. Zhu, J. Pfeifer, A. Bax, NMRPipe: a multidimensional spectral processing system based on UNIX pipes, J. Biomol. NMR 6 (1995) 277–293.
[16] D.G. Kneller, I.D. Kuntz, UCSF sparky – an NMR display, annotation and assignment tool, J. Cell. Biochem. (1993) (254–254).
[17] Y. Shen, F. Delaglio, G. Cornilescu, A. Bax, TALOS+: a hybrid method for predicting protein backbone torsion angles from NMR chemical shifts, J. Biomol. NMR 44 (2009) 213–223.
[18] C.D. Schwieters, J.J. Kuszewski, N. Tjandra, G. Marius Clore, The Xplor-NIH NMR molecular structure determination package, J. Magn. Reson. 160 (2003) 65–73.
[19] R.A. Laskowski, J.A. Rullmannn, M.W. MacArthur, R. Kaptein, J.M. Thornton, AQUA and PROCHECK-NMR: programs for checking the quality of protein structures solved by NMR, J. Biomol. NMR 8 (1996) 477–486.
[20] R. Koradi, M. Billeter, K. Wuthrich, MOLMOL: a program for display and analysis of macromolecular structures, J. Mol. Graph. 14 (51–55) (1996) 29–32.
[21] R.A. Laskowski, PDBsum: summaries and analyses of PDB structures, Nucleic Acids Res. 29 (2001) 221–222.
[22] H. Li, Y. Bi, B. Xia, C. Jin, ^{1}H, ^{13}C and ^{15}N resonance assignments of the rhodanese domain of YgaP from *Escherichia coli*, Biomol. NMR Assign 5 (2011) 101–103.
[23] F. Sievers, A. Wilm, D. Dineen, T.J. Gibson, K. Karplus, W.Z. Li, R. Lopez, H. McWilliam, M. Remmert, J. Soding, J.D. Thompson, D.G. Higgins, Fast, scalable generation of high-quality protein multiple sequence alignments using Clustal Omega, Mol. Syst. Biol. 7 (2011).
[24] X. Robert, P. Gouet, Deciphering key features in protein structures with the new ENDscript server, Nucleic Acids Res. 42 (2014) W320–324.
[25] L. Holm, S. Kaariainen, P. Rosenstrom, A. Schenkel, Searching protein structure databases with DaliLite v. 3, Bioinformatics 24 (2008) 2780–2781.
[26] A.G. Palmer 3rd, NMR characterization of the dynamics of biomacromolecules, Chem. Rev. 104 (2004) 3623–3640.